

Mechanism of the Nucleophilic Substitution of Acyl Electrophiles using Lithium Organocuprates

Naohiko Yoshikai,^a Ryoko Iida,^a and Eiichi Nakamura^{a,*}

^a Department of Chemistry, The University of Tokyo, Bunkyo-ku, Tokyo 113-0033, Japan
Fax: (+81)-3-5800-6889; e-mail: nakamura@chem.s.u-tokyo.ac.jp

Received: January 26, 2008; Published online: April 15, 2008

This paper is dedicated to Prof. Andreas Pfaltz, my long-time best friend, on the occasion of his 60th birthday, in honor of his outstanding contribution to the field of transition metal catalysis.



Supporting information for this article is available on the WWW under <http://asc.wiley-vch.de/home/>.

Abstract: The mechanism of nucleophilic substitution reaction at an sp^2 carbon center of a thioester or an acid chloride with a lithium organocuprate reagent has been investigated. Density functional calculations indicated that the thioester undergoes oxidative addition of the C–S bond to the copper(I) atom through a three-centered transition state to afford an organocopper(III) intermediate, which gives the product through reductive elimination of the alkyl and the acyl groups. On the other hand, the acid chloride loses a chloride anion very easily when it interacts with the cuprate, because the chloride

anion is captured by a lithium(I) cation rather than a copper(I) atom. ^{13}C kinetic isotope effect (KIE) experiments showed excellent agreement with computational predictions for the thioester reaction, but suggested that the nucleophilic displacement transition state of the acid chloride occurs much more advanced than the calculations predict.

Keywords: cuprates; density functional calculations; isotope effects; nucleophilic substitution; reaction mechanisms

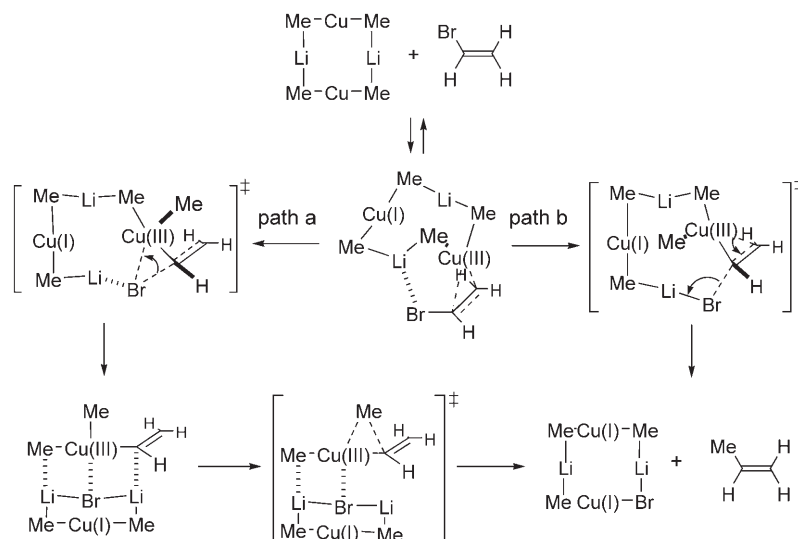
Introduction

Nucleophilic substitution of a carboxylic acid chloride, or its equivalent, with an organometallic reagent is one of the most basic methods used to synthesize ketones.^[1,2] While organozinc reagents were the first organometallic reagents employed in such transformations, they quickly fell out of favor because of their extremely limited scope.^[3] On the other hand, since the first report by Gilman in 1936^[4] followed more recently by Whitesides in 1967,^[5] organocopper reagents, and organocuprate reagents (R_2CuLi) in particular, have shown a much wider scope in the substitution of acid chlorides.^[6] The mild, yet sufficient, nucleophilicity of organocuprates allows a high compatibility with functional groups such as ketones, nitriles, and esters, and they can be used in the synthesis of a variety of natural products.^[7] Shortly after the reports on the acid chloride reaction, Rosenblum et al. reported on the substitution of a thioester with an organocuprate.^[8] This reaction further expanded the utility of organocopper reagents in ketone synthesis, since classical organozinc reagents do not undergo a dis-

placement of the C–S bond. While the catalytic variants developed later have overridden stoichiometric cuprate acylation,^[9,10] it still finds applications as a highly reliable transformation.^[11]

Despite its synthetic utility, the mechanism of organocuprate reactions with acyl electrophiles has not been studied, while other organocopper transformations, such as conjugate additions and alkylation reactions, have been extensively studied by both our^[12,13] and other research groups.^[12,14] These studies suggest that the mechanism of the acylation of R_2CuLi is not merely a simple “addition-elimination” sequence of the R^- anion, but involves a Cu(I)/Cu(III) redox process.

An organocuprate transformation related to these acylation reactions would be the substitution of an alkyl halide.^[15] Our recent study on this reaction suggested two mechanisms of the halide displacement on the sp^2 carbon atom (Scheme 1).^[16] One mechanism involves an insertion of the copper(I) atom into the carbon-halogen bond followed by the reductive elimination of the resulting organocopper(III) intermediate (a three-centered mechanism, path a). In the



Scheme 1. The two pathways for the substitution of vinyl bromide with lithium organocuprate.

other mechanism, the halide anion eliminates by itself without an interaction with the copper atom, and is trapped by the lithium cation (an eliminative mechanism, path b). Experimental measurements and theoretical predictions of the $^{12}\text{C}/^{13}\text{C}$ kinetic isotope effect indicate that the latter mechanism occurs in the actual reaction.

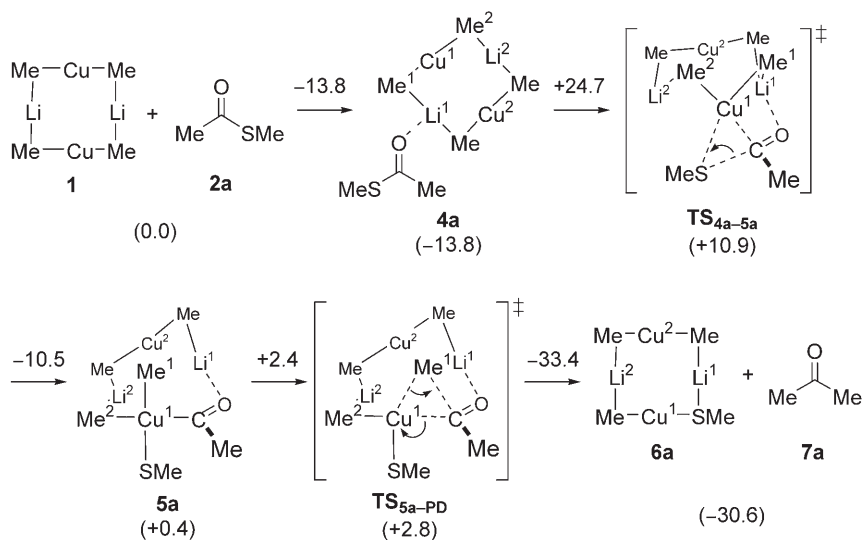
We envisioned that such a mechanistic dichotomy (i.e., a three-centered versus eliminative mechanism) could also exist in the substitution reaction on the sp^2 carbon atom of acyl electrophiles. In this paper, we report on theoretical and experimental studies on the nucleophilic substitution reactions of a thioester and an acid chloride with a lithium organocuprate. The reaction pathways of these electrophiles turned out to

be entirely different from each other. Thus, the reaction of the thioester involves a three-centered oxidative addition/reductive elimination sequence, while the acid chloride follows the eliminative reaction pathway. The origin of the contrasting reaction pathways will be discussed in more detail.

Results and Discussion

Reaction of $[\text{Me}_2\text{CuLi}]_2$ and *S*-Methyl Thioacetate

First, we examined the reaction pathway for the substitution of *S*-methyl thioacetate (**2a**) with $[\text{Me}_2\text{CuLi}]_2$ (**1**) (Scheme 2, Figure 1). The dimeric organocuprate



Scheme 2. Reaction pathway for the substitution of *S*-methyl thioacetate with $[\text{Me}_2\text{CuLi}]_2$. Values in parentheses refer to the potential energy (in kcal mol^{-1}) relative to (**1** + **2a**). The change in energy is shown above the reaction arrows.

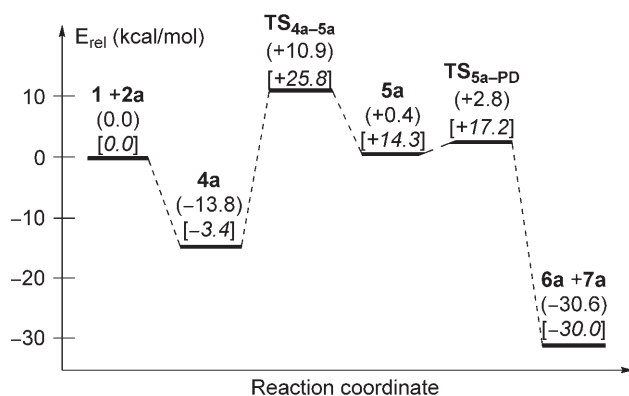


Figure 1. Potential energy profile (in kcal mol⁻¹) for the substitution of *S*-methyl thioacetate with [Me₂CuLi]₂. Values in *italics* refer to the Gibbs free energies (kcal mol⁻¹) at 298 K.

1 and **2a** initially form the complex **4a** by an interaction between the lithium and the oxygen atoms ($\Delta E = 13.8$ kcal mol⁻¹). Complex **4a** then undergoes oxidative addition of the C–S bond to the copper atom through a three-centered transition state (TS) ($\Delta E^\ddagger = 24.7$ kcal mol⁻¹ for TS_{4a-5a}) to give the square-planar acyldimethylcopper(III) intermediate **5a**. The subsequent reductive elimination of the methyl and the acyl groups (TS_{5a-PD}) occurs smoothly with an activation energy of 2.4 kcal mol⁻¹. The overall process is expectedly highly exothermic (–30.6 kcal mol⁻¹). Note that an eliminative TS for the C–S bond cleavage (such as path b in Scheme 1) was not found. The strong affinity of the sulfur atom for the copper atom should make the eliminative mode of the C–S cleavage much more unfavorable than the three-centered mode (i.e., TS_{4a-5a}).

The structures of the complexes and the TS are shown in Figure 2. The C–S bond substantially elongates on passing from complex **4a** to TS_{4a-5a} (a 20% increase from 1.77 to 2.13 Å), and the forming Cu–C (acyl) (1.97 Å) and the Cu–S (2.37 Å) bond distances in TS_{4a-5a} are very close to those in the oxidative addition product **5a** (Cu–C = 1.93 Å and Cu–S = 2.32 Å). Natural population analysis indicates a formal oxidation of the Cu atom (+0.44 in **4a** and +0.86 in **5a**) and the displacement of the SMe group as a thiolate anion (+0.26 in **4a** and –0.50 in **5a**). The structures of the Cu(III) intermediate **5a** and its reductive elimination TS (TS_{5a-PD}) are similar to the related cases.^[12–14]

Based on the above reaction pathway, we examined the effect of solvent coordination to the lithium atom using the model complex **1**·2S (S = Me₂O). As shown in Scheme 3, the reaction pathway is essentially the same as the reaction pathway without any coordinating solvent molecules (Scheme 2) except for the presence of a π -complex **4a'**·2S. First, the complex **4a**·2S forms through a lithium–oxygen interaction with a sta-

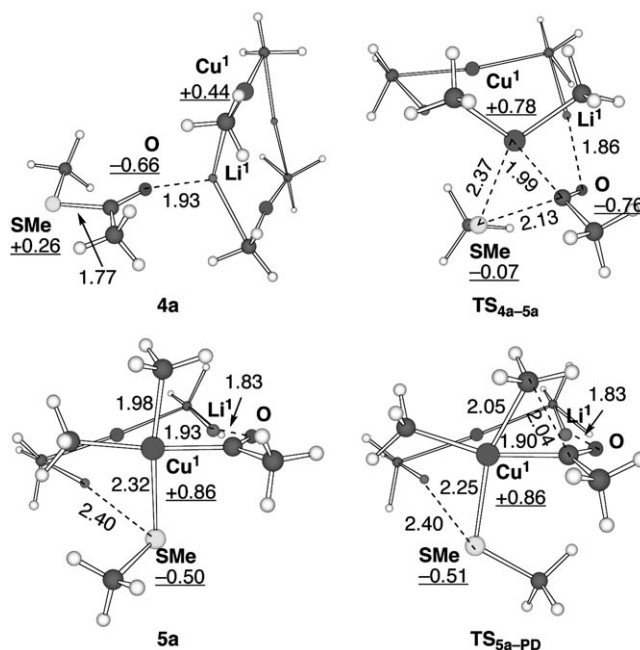
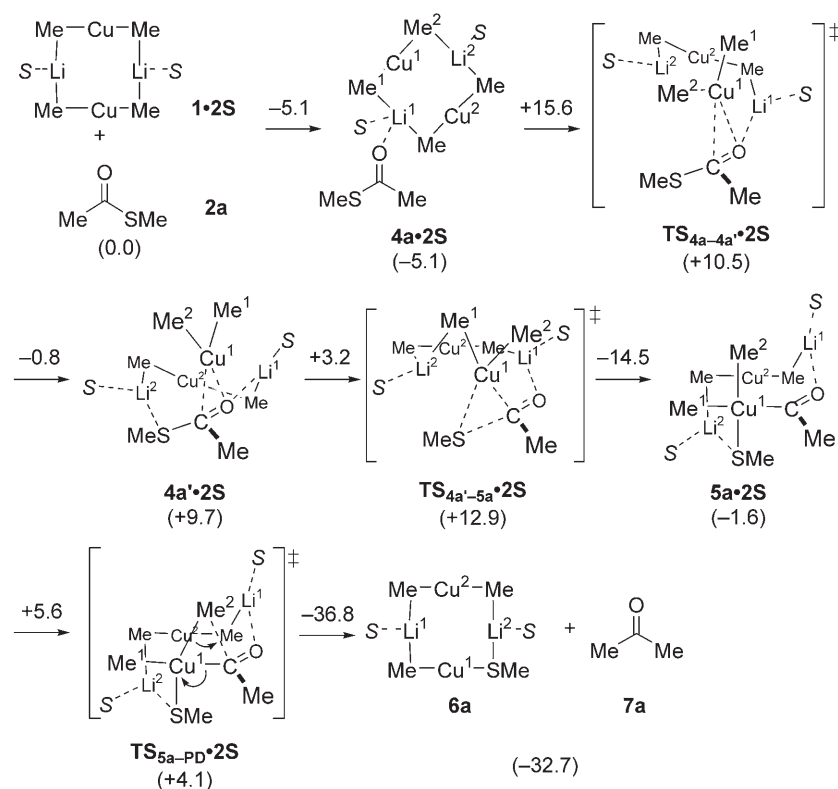


Figure 2. Structure of the complexes and the TS in the reaction of [Me₂CuLi]₂ and *S*-methyl thioacetate. The values refer to the bond lengths in Å (plain text) and natural charges (underlined).

bilization of 5.1 kcal mol⁻¹. Then, the Cu atom approaches the C=O bond to form the π -complex **4a'**·2S through TS_{4a-4a'·2S ($\Delta E^\ddagger = 15.6$ kcal mol⁻¹). This process is endothermic by 14.8 kcal mol⁻¹. The π -complex **4a'**·2S undergoes three-centered oxidative addition of the C–S bond to the Cu atom (TS_{4a'-5a}·2S, $\Delta E^\ddagger = 3.2$ kcal mol⁻¹) to form a square-planar Cu(III) intermediate **5a**·2S. The triorganocopper(III) intermediate **5a**·2S smoothly undergoes reductive elimination (TS_{5a-PD}·2S, $\Delta E^\ddagger = 5.6$ kcal mol⁻¹) to give the final products. The energy profile of the overall pathway (Figure 3) indicates that the C–S bond cleavage is the rate-determining step of the reaction.}

The structure of the intermediates and the TS are shown in Figure 4. Upon π -complexation, both the C–S and the C–O bonds elongate (C–S bond = 1.77 Å in **4a**·2S and 1.86 Å in **4a'**·2S, and the C–O bond = 1.22 Å in **4a**·2S and 1.33 Å in **4a'**·2S). In a parallel manner, the Li–O (acyl) bond distance becomes considerably shorter (2.01 Å in **4a**·2S and 1.82 Å in **4a'**·2S). These structural changes should reflect the back-donation from the Cu atom to the C=O $\pi^*/$ C–S σ^* mixed orbital. In fact, the positive charge on the Cu atom increases (+0.42 to +0.92), while the negative charges increase on the carbonyl oxygen (–0.65 to –0.87), the carbonyl carbon (+0.41 to 0.00) and the SMe group (+0.26 to +0.02). The oxidative addition TS (TS_{4a'-5a}·2S) takes a similar structure to the TS without any Me₂O molecules (see TS_{4a-5a} in Figure 2)



Scheme 3. Reaction pathway for the substitution of *S*-methyl thioacetate with $[\text{Me}_2\text{CuLi}]_2 \cdot 2\text{S}$ ($\text{S} = \text{Me}_2\text{O}$). Values in parentheses refer to the potential energy (in kcal mol^{-1}) relative to $(\mathbf{1} \cdot 2\text{S} + \mathbf{2a})$. The change in energy is shown above the reaction arrows.

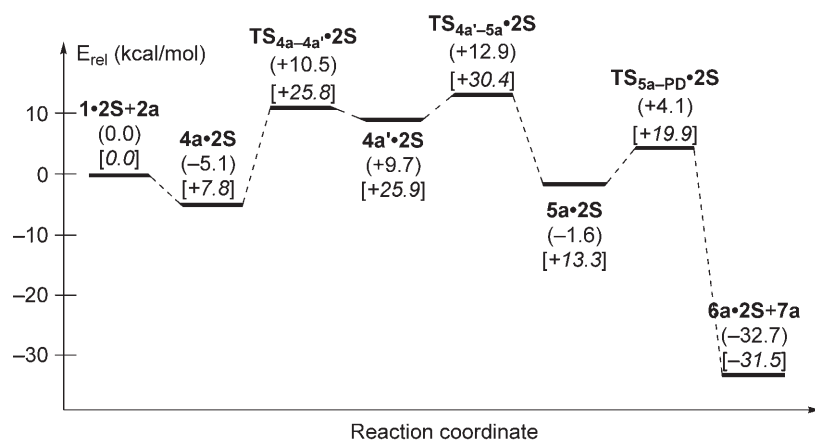


Figure 3. Potential energy profile (in kcal mol^{-1}) for the substitution of *S*-methyl thioacetate with $[\text{Me}_2\text{CuLi}]_2 \cdot 2\text{S}$ ($\text{S} = \text{Me}_2\text{O}$). Values in italic refer to the Gibbs free energies (kcal mol^{-1}) at 298 K.

except for the small difference in the Cu–S and Li–S bond distances (Cu–S = 2.46 Å versus 2.37 Å, and Li–S = 2.75 Å versus 3.07 Å). The structures of the resulting Cu(III) intermediate, $\mathbf{5a} \cdot 2\text{S}$, and the following reductive elimination TS ($\text{TS}_{5a\text{-PD}} \cdot 2\text{S}$) are very close to those without any coordinating solvents (Figure 2).

Reaction of $[\text{Me}_2\text{CuLi}]_2$ and Acetyl Chloride

Next, we examined the reaction pathway for the substitution of acetyl chloride ($\mathbf{3a}$) with $[\text{Me}_2\text{CuLi}]_2$ ($\mathbf{1}$) (Scheme 4, Figure 5). First, the dimeric organocuprate $\mathbf{1}$ and $\mathbf{3a}$ form a complex $\mathbf{8a}$ through the lithium–oxygen interaction having a stabilization energy of $9.4 \text{ kcal mol}^{-1}$. Complexation between the Cu atom

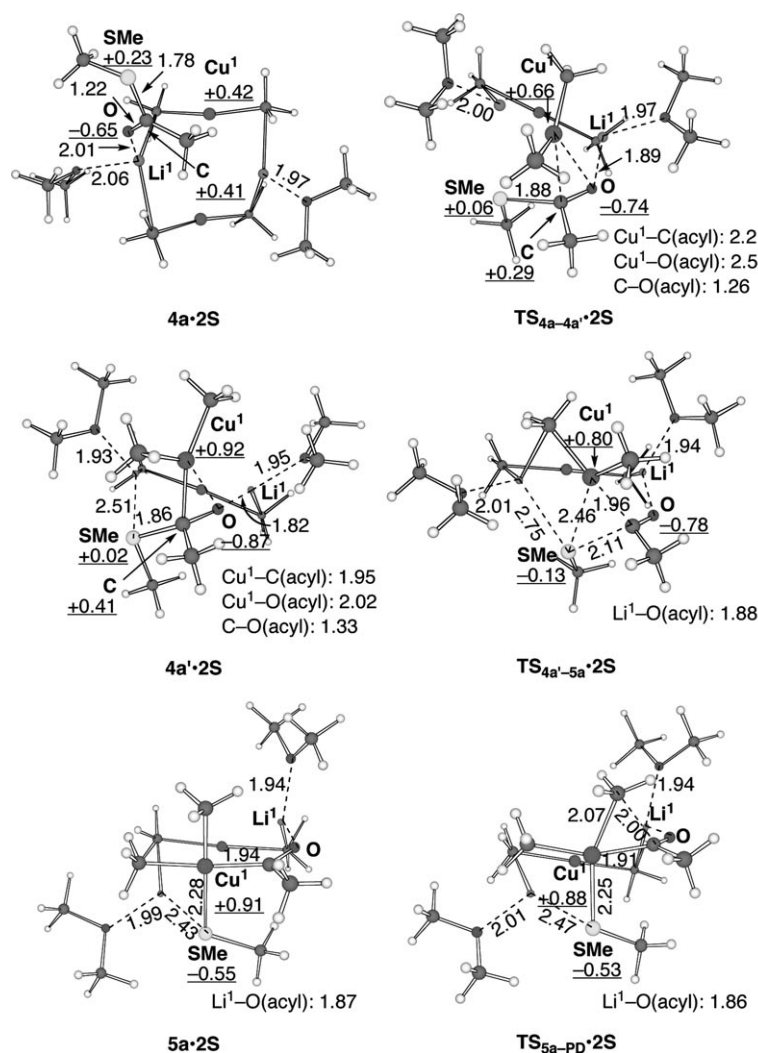
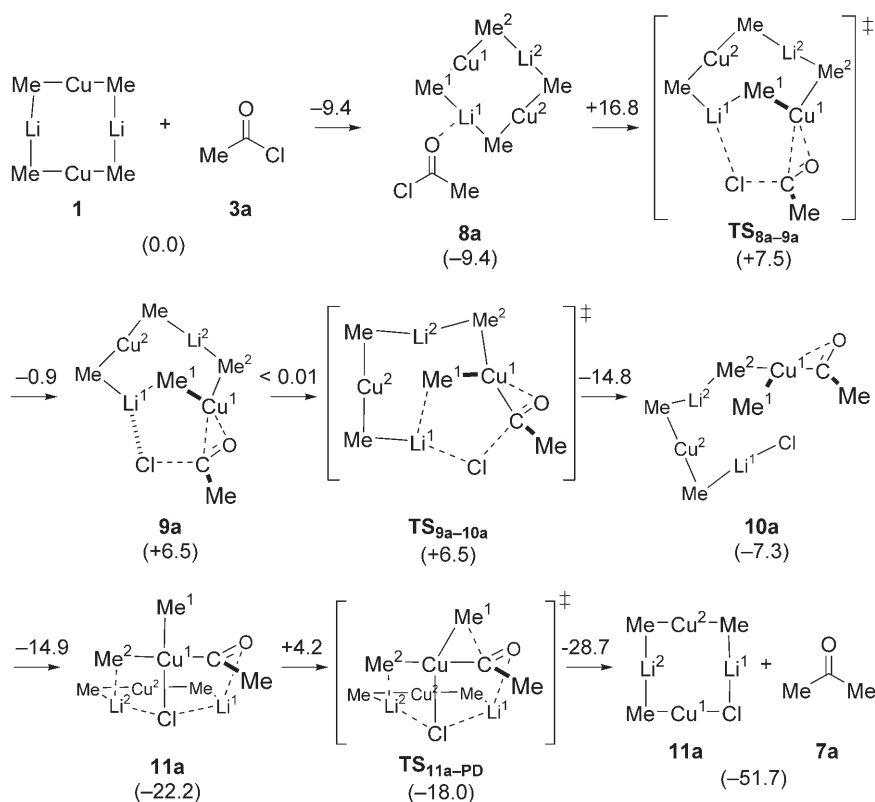


Figure 4. Structure of complexes and TS in the reaction of $[\text{Me}_2\text{CuLi}]_2 \cdot 2\text{S}$ and *S*-methyl thioacetate. The values refer to the bond lengths in Å (plain text) and natural charges (underlined).

and the C=O bond takes place through TS_{8a-9a} with an activation energy of $16.8 \text{ kcal mol}^{-1}$ to give the π -complex **9a**. The formation of **9a** from **8a** is endothermic by $15.9 \text{ kcal mol}^{-1}$. The π -complex **9a** undergoes a practically spontaneous C–Cl bond cleavage through an eliminative TS (TS_{9a-10a}). The potential surface around the C–Cl bond cleavage is extremely flat, and the calculated activation barrier is low at $0.006 \text{ kcal mol}^{-1}$. The eliminative C–Cl bond cleavage leads to the formation of the triorganocopper(III) intermediate **10a**. Rearrangement of the complex **10a** gives a more stable copper(III) complex **11a**, which undergoes facile reductive elimination through TS_{11a-PD} ($\Delta E^\ddagger = 4.2 \text{ kcal mol}^{-1}$) to give the final products. The overall transformation is expectedly highly exothermic ($-46.7 \text{ kcal mol}^{-1}$). Note that all attempts to locate a three-centered insertion TS (such as TS_{4a-5a} in Scheme 2) were unsuccessful.

The structure of the intermediates and TS are shown in Figure 6. The C–Cl bond elongates considerably on π -complex formation (an increase of 20%, 1.79 Å in **8a** and 2.15 Å in **9a**). Accordingly, both the negative charge on the Cl atom (-0.03 in **8a** and -0.42 in **9a**) and the positive charge on the Cu atom ($+0.44$ in **8a** and $+0.84$ in **9a**) increase. In accordance with the extremely low activation barrier for the C–Cl bond cleavage, the structural changes on passing from **9a** to TS_{9a-10a} are very small. For example, the C–Cl bond length increases by only 2% (2.15 Å to 2.20 Å). The acyldimethylcopper complex **10a** has a highly distorted square-planar structure, where the carbonyl oxygen acts as an internal ligand to the Cu(III) center. The coordination of the carbonyl oxygen is indicated by the short Cu–O bond distance (2.29 Å) and the small Cu–C–O bond angle (92.6°). On the other hand, in the other acyldimethylcopper intermediate, **11a**, the chloride anion serves as a



Scheme 4. Reaction pathway for the substitution of acetyl chloride with $[\text{Me}_2\text{CuLi}]_2$. Values in parentheses refer to the potential energy (in kcal mol^{-1}) relative to $(\mathbf{1} + \mathbf{3a})$. The change in energy is shown above the reaction arrows.

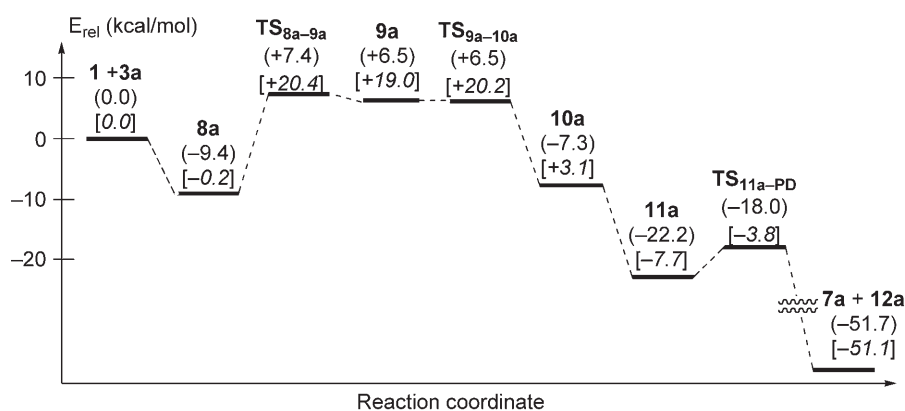


Figure 5. Potential energy profile (in kcal mol^{-1}) for the substitution of acetyl chloride with $[\text{Me}_2\text{CuLi}]_2$. Values in italic refer to the Gibbs free energy (kcal mol^{-1}) at 298 K.

ligand to Cu(III) ($\text{Cu}-\text{Cl}=2.35 \text{ \AA}$) to form the square-planar structure, and the oxygen atom lies out of the plane. This structural arrangement is suitable for the reductive elimination ($\text{TS}_{11a\text{-PD}}$), where the $\text{C}=\text{O}$ π orbital can participate in the formation of a $\text{C}-\text{C}$ bond.^[13]

Based on the above reaction pathway, we examined the effect of solvent coordination to the lithium atoms using the model complex $\mathbf{1}\cdot\mathbf{2S}$. However, all attempts to locate a π -complex or a transition state for

$\text{C}-\text{Cl}$ bond cleavage failed. Thus, approaches of the Cu atom to the $\text{C}=\text{O}$ bond and the Li atom to the Cl atom result in a spontaneous cleavage of the $\text{C}-\text{Cl}$ bond. A theoretical study on an extremely fast organic reaction tends to result in a very flat potential energy surface, and sometimes even in the absence of a saddle point.^[17] Considering that the reaction of the acid chloride is almost instantaneous, the absence of the potential energy barrier for the present case is not very surprising. As discussed in more detail later, we

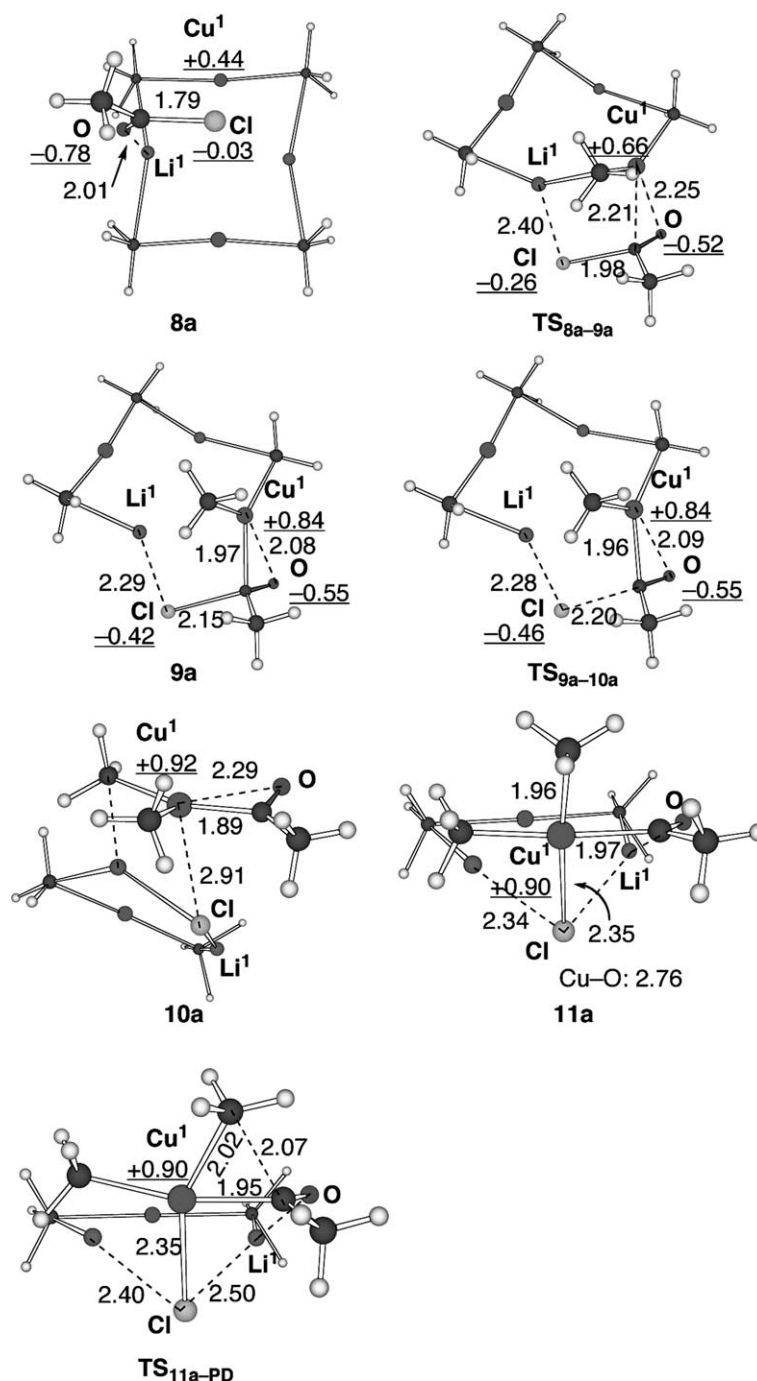


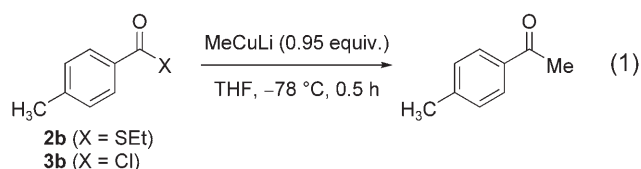
Figure 6. Structure of intermediates and TS in the reaction of $[\text{Me}_2\text{CuLi}]_2$ and acetyl chloride. The values refer to the bond lengths in Å (plain text) and natural charges (underlined).

speculate that the spontaneous collapse of the acid chloride is a sign of a late nature of the actual C–Cl bond cleavage TS.

Kinetic Isotope Effect Studies

To obtain further information on the C–X bond cleavage (oxidative addition) step in the above substi-

tution reactions, we carried out measurements of the $^{12}\text{C}/^{13}\text{C}$ kinetic isotope effect (KIE) using quantitative ^{13}C NMR analysis (see Supporting Information for experimental details).^[16,18] Thus, the reaction of the thioester **2b** and the acid chloride **3b** with Me_2CuLi was performed to a 93% and 86% conversion, respectively [Eq. (1)], and the unreacted starting material was recovered from the reaction mixture. The $^{12}\text{C}/^{13}\text{C}$ KIE data were calculated from a comparison of the ^{13}C in-



tegrations of the starting and the recovered materials. Note that, in the case of the acid chloride **3b**, the reaction was quenched by the addition of MeOH, and the unreacted material was recovered as the corresponding methyl ester. The *para*-methyl carbon atom was taken as the internal standard for the ^{13}C NMR integration.

The experimental KIE values are shown in Figure 7. In both cases, a significant KIE value was found on the carbonyl carbon atom (1.034 for **2b** and 1.024 for **3b**), while the KIE values on the other carbon atoms were either negligible or very small (1.001–1.005). Thus, these KIE profiles should reflect the C–X bond cleavage step as the rate-determining step of the reaction.

To evaluate the reaction pathways obtained by the above theoretical studies, the $^{12}\text{C}/^{13}\text{C}$ KIE values in the C–X bond cleavage TS were calculated for both the model and the real substrates (i.e., **2a/2b** and **3a/3b**). Figure 8 shows the calculated KIE values in the C–S bond cleavage step for the model substrate **2a** and the real substrate **2b**. The KIE value on the carbonyl carbon atom of **2a** was *ca.* 1.050 for both the non-solvated (TS_{4a-5a} in Figure 8a) and the solvated ($\text{TS}_{4a'-5a'}\cdot 2\text{S}$, Figure 8b) models, and much larger than the experimental value (1.034). Note that the similar KIE values for TS_{4a-5a} and $\text{TS}_{4a'-5a'}\cdot 2\text{S}$ would come from their similar three-centered structure (especially the C–S bond length, see Figure 2 and Figure 4). On the other hand, the corresponding KIE value for the real substrate **2b** (1.034, Figure 8c) was in excellent agreement with the experimental value (1.034, Figure 7). The significant difference in the KIE values for the model and the real substrates reflects the structural difference in the C–S bond cleavage TSs (TS_{4a-5a} vs. TS_{4b-5b} ; see Figure 2 and Figure 8d). Thus, TS_{4b-5b} can be regarded as being a much later TS than TS_{4a-5a} as seen from the much more advanced C–S bond cleavage (C–S bond length = 2.13 Å in TS_{4a-5a} and 2.52 Å in TS_{4b-5b} , and the natural charge on the SR group is –0.07 in TS_{4a-5a} and –0.28 in TS_{4b-5b}).

Figure 9 shows the calculated KIE values of the C–Cl bond cleavage step for the model substrate **3a** (TS_{9a-10a}) and the real substrate **3b** (TS_{9b-10b}). The KIE values on the carbonyl carbon were 1.053 and 1.051 for TS_{9a-10a} and TS_{9b-10b} , respectively. The similar magnitude of the KIE values for TS_{9a-10a} and TS_{9b-10b} is in accordance with their similar structures and charge distributions (see Figure 6 and Figure 9c). These values are much larger than the experimental value (1.024, Figure 7).

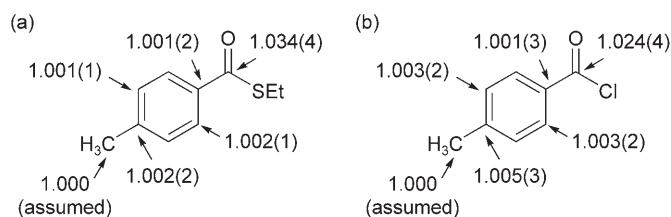


Figure 7. Experimental $^{12}\text{C}/^{13}\text{C}$ KIE values for: (a) the substitution of thioester **2b** and (b) acid chloride **3b** with Me_2CuLi . The values in the parentheses indicate experimental errors in the last digit.

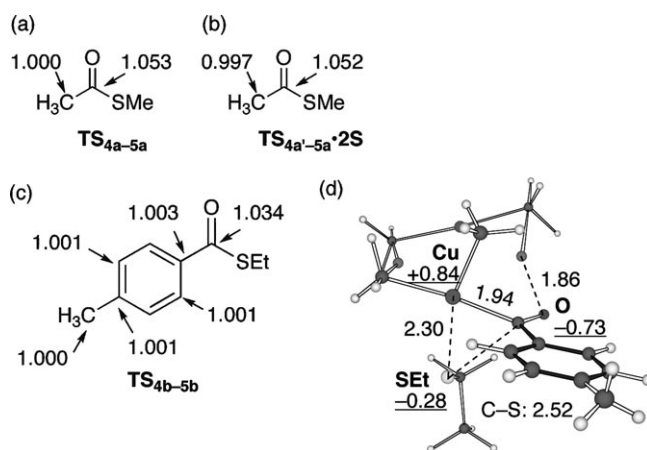


Figure 8. (a)–(c) Calculated $^{12}\text{C}/^{13}\text{C}$ KIE values for the C–S bond cleavage TS (a = TS_{4a-5a} , b = $\text{TS}_{4a'-5a'}\cdot 2\text{S}$, and c = TS_{4b-5b}) and (d) structure of TS_{4b-5b} .

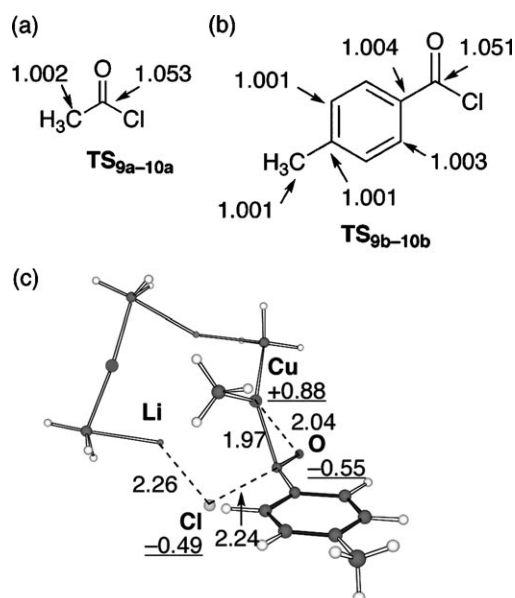
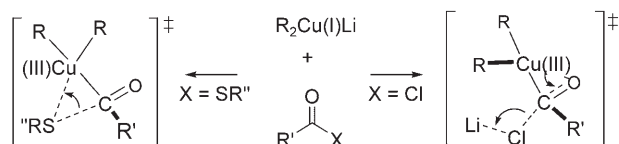


Figure 9. (a) and (b) Calculated $^{12}\text{C}/^{13}\text{C}$ KIE values for the C–Cl bond cleavage TS (a = TS_{9a-10a} and b = TS_{9b-10b}) and (c) the structure of TS_{9b-10b} .



Scheme 5. Mechanisms of the oxidative addition of acyl C–S and C–Cl bonds to organocuprates.

The considerable discrepancy between the experimental and the calculated KIE values should be the problem of the computational side, that is, the insufficient model and method (e.g., the absence of ethereal solvent molecule), which should have led to the inappropriate estimation of the degree of the C–Cl bond cleavage. The smaller experimental KIE value than the calculated one suggests two mechanistic possibilities.^[19] Thus, the C–Cl bond cleavage in the actual transition state is much less advanced (i.e., early TS) or much more advanced (i.e., late TS) than predicted by the calculation. We think that the latter possibility is more likely in light of the following points: (1) The reaction of the acid chloride with the organocuprate takes place almost instantaneously, (2) The unsolvated organocuprate model (**1**) gives the extremely flat potential surface of the C–Cl bond cleavage (Figure 5) and the solvated model (**1·2 S**) effects the spontaneous collapse of the acid chloride, and (3) the potential surface analysis of an extremely fast reaction often underestimates the degree of the bond reorganization in the actual transition state.^[17]

Conclusions

In summary, we have addressed the mechanisms of nucleophilic substitution reactions to acyl electrophiles, such as thioesters and acid chlorides, using a lithium organocuprate. Computations and experimental studies indicate that the reaction of a thioester takes place through a three-centered oxidative addition of the C–S bond to the Cu atom, while an acid chloride undergoes eliminative C–Cl bond cleavage through Lewis acid activation of the Cl atom with the Li atom (Scheme 5). Such mechanistic differences originate from the nature of the leaving group. The thioester favors a three-centered pathway due to the strong affinity of the “soft” thiolate anion to the “soft” copper atom. On the other hand, the “hard” chloride anion prefers to interact with the “hard” lithium cation, and making the eliminative pathway more feasible. Finally, this study shows that the dichotomy of the “three-centered” and “eliminative” pathways is a critical issue in explorations into the mechanism of the oxidative addition of a C(sp^2)–X bond to a d^{10} or related transition metal complex,^[16] and in the design of a catalytic cycle involving such an elementary process.^[20]

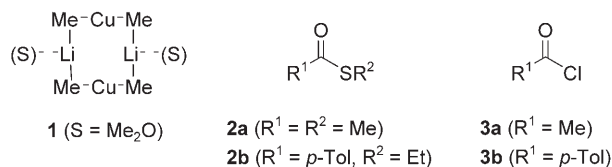


Figure 10. Chemical models used in the computational studies on the substitution reactions of thioesters and acid chlorides with organocuprates.

Experimental Section

Computational Methods and Models

All the calculations were performed using the Gaussian 03 program package.^[21] Density functional theory (DFT) was employed using the B3LYP hybrid functional.^[22] The structures were optimized using a basis set (denoted as 631SDD) consisting of the SDD basis set consisting of a double- ζ valence basis set and the Stuttgart–Dresden effective core potential (ECP) for Cu,^[23] and the 6–31G(d) basis set^[24] for the remaining atoms. The method and the basis sets used here are known to give reliable results for the structure and reactivity of organocuprate reagents.^[25] Stationary points were adequately characterized using normal coordinate analysis. Intrinsic reaction coordinate (IRC) analysis^[26] was carried out for the major reaction pathway to confirm that all the stationary points were smoothly connected to each other. The kinetic isotope effect (KIE) was calculated using Bigeleisen–Mayer’s equation^[27] with the Wigner tunnel correction using frequencies scaled by a factor of 0.9614.^[28] Natural population analysis was performed at the same level as that used for the geometry optimization.^[29]

We employed dimeric lithium dimethyl cuprate [Me_2CuLi]₂ (**1**) as the model organocuprate, and *S*-methyl thioacetate (**2a**) and acetyl chloride (**3a**) as model substrates (Figure 10). The effect of the coordination of the ethereal solvent was modeled by a single Me_2O molecule on the lithium atom (**1·2 S**). The critical step (i.e., the displacement of the leaving group) of the reaction of *S*-ethyl *p*-methylbenzothioate (**2b**) or *p*-toluoyl chloride (**3b**) was also studied to evaluate the experimental KIE data.

Acknowledgements

We wish to thank the Ministry of Education, Culture, Sports, Science and Technology of Japan for financial support (Grant-in-Aid for scientific research (No. 18105004 for E.N and No. 19029008 for N.Y.) and Global COE Program for Chemistry Innovation).

References

- [1] *Comprehensive Organic Transformations*, 2nd edn., (Ed.: R. C. Larock), Wiley-VCH, Weinheim, **1999**.
- [2] R. K. Dieter, *Tetrahedron* **1999**, *55*, 4177–4236.
- [3] D. A. Shirley, *Org. React.* **1958**, *8*, 28–58.

- [4] H. Gilman, J. M. Straley, *Recl. Trav. Chim. Pays-Bas* **1936**, 55, 821.
- [5] G. M. Whitesides, C. P. Casey, J. San Filippo Jr, E. Panek, *Trans. N. Y. Acad. Sci.* **1967**, 29, 572–574.
- [6] a) G. H. Posner, C. E. Whitten, *Tetrahedron Lett.* **1970**, 53, 4647–4650; b) C. Jallabert, N. T. Luong-Thi, H. Riviere, *Bull. Soc. Chim. Fr.* **1970**, 797–798; c) G. H. Posner, C. E. Whitten, P. McFarland, *J. Am. Chem. Soc.* **1972**, 94, 5106–5108.
- [7] a) S. Masamune, M. Hiram, S. Mori, S. A. Ali, D. S. Garvey, *J. Am. Chem. Soc.* **1981**, 103, 1568–1571; b) P. R. McGuirk, D. B. Collum, *J. Am. Chem. Soc.* **1982**, 104, 4496–4497; c) D. V. Patel, F. VanMiddlesworth, J. Donaubaauer, P. Gannett, C. J. Sih, *J. Am. Chem. Soc.* **1986**, 108, 4603–4614.
- [8] R. J. Anderson, C. A. Henrick, L. D. Rosenblum, *J. Am. Chem. Soc.* **1974**, 96, 3654–3655.
- [9] *Metal-catalyzed Cross-coupling Reactions*, 2nd edn., (Ed.: A. deMeijere, F. Diederich), Wiley-VCH, New York, **2004**.
- [10] For example: a) H. Tokuyama, S. Yokoshima, T. Yamashita, T. Fukuyama, *Tetrahedron Lett.* **1998**, 39, 3189–3192; b) Y. Zhang, T. Rovis, *J. Am. Chem. Soc.* **2004**, 126, 15964–15965; c) H. Yang, H. Li, R. Wittenberg, M. Egi, W. Huang, L. S. Liebeskind, *J. Am. Chem. Soc.* **2007**, 129, 1132–1140; d) J. M. Villalobos, J. Srogl, L. S. Liebeskind, *J. Am. Chem. Soc.* **2007**, 129, 15734–15735.
- [11] a) W. Zhang, R. G. Carter, A. F. T. Yokochi, *J. Org. Chem.* **2004**, 69, 2569–2572; b) W. Zhang, R. G. Carter, *Org. Lett.* **2005**, 7, 4209–4212.
- [12] a) E. Nakamura, S. Mori, *Angew. Chem.* **2000**, 112, 3902–3924; *Angew. Chem. Int. Ed.* **2000**, 39, 3750–3771; b) E. Nakamura, N. Yoshikai, *Bull. Chem. Soc. Jpn.* **2004**, 77, 1–11, and references cited therein.
- [13] a) E. Nakamura, S. Mori, M. Nakamura, K. Morokuma, *J. Am. Chem. Soc.* **1997**, 119, 4887; b) E. Nakamura, S. Mori, K. Morokuma, *J. Am. Chem. Soc.* **1997**, 119, 4900; c) E. Nakamura, S. Mori, K. Morokuma, *J. Am. Chem. Soc.* **1998**, 120, 8273; d) S. Mori, E. Nakamura, *Chem. Eur. J.* **1999**, 5, 1534; e) E. Nakamura, M. Yamana, *J. Am. Chem. Soc.* **1999**, 121, 8941–8942; f) S. Mori, E. Nakamura, K. Morokuma, *J. Am. Chem. Soc.* **2000**, 122, 7294; g) E. Nakamura, M. Yamana, N. Yoshikai, S. Mori, *Angew. Chem.* **2001**, 113, 1989–1992; *Angew. Chem. Int. Ed.* **2001**, 40, 1935–1938; h) M. Yamana, E. Nakamura, *Organometallics* **2001**, 20, 5675; i) M. Yamana, S. Kato, E. Nakamura, *J. Am. Chem. Soc.* **2004**, 126, 6287–6293; j) M. Yamana, E. Nakamura, *J. Am. Chem. Soc.* **2005**, 127, 4697–4706.
- [14] For recent literature: a) S. H. Bertz, S. Cope, D. Dorton, M. Murphy, C. A. Ogle, *Angew. Chem.* **2007**, 119, 7212–7215; *Angew. Chem. Int. Ed.* **2007**, 46, 7082–7085; b) S. H. Bertz, S. Cope, M. Murphy, C. A. Ogle, B. J. Taylor, *J. Am. Chem. Soc.* **2007**, 129, 7208–7209; c) T. Gärtner, W. Henze, R. M. Gschwind, *J. Am. Chem. Soc.* **2007**, 129, 11362–11363.
- [15] E. J. Corey, G. H. Posner, *J. Am. Chem. Soc.* **1967**, 89, 3911.
- [16] N. Yoshikai, E. Nakamura, *J. Am. Chem. Soc.* **2004**, 126, 12264–12265.
- [17] a) A. E. Keating, S. R. Merrigan, D. A. Singleton, K. N. Houk, *J. Am. Chem. Soc.* **1999**, 121, 3933–3938; b) D. T. Nowlan III, D. A. Singleton, *J. Am. Chem. Soc.* **2005**, 127, 6190–6191.
- [18] a) D. A. Singleton, A. A. Thomas, *J. Am. Chem. Soc.* **1995**, 117, 9357–9358; b) D. E. Frantz, D. A. Singleton, J. P. Snyder, *J. Am. Chem. Soc.* **1997**, 119, 3383–3384.
- [19] L. C. S. Melandar, W. H. Saunders, *Reaction Rates of Isotopic Molecules*, Wiley, New York, **1980**.
- [20] N. Yoshikai, H. Mashima, E. Nakamura, *J. Am. Chem. Soc.* **2005**, 127, 17978–17979.
- [21] M. J. Frisch, G. W. Trucks, H. B. Schlegel, G. E. Scuseria, M. A. Robb, J. R. Cheeseman, J. A. Montgomery, Jr., T. Vreven, K. N. Kudin, J. C. Burant, J. M. Millam, S. S. Iyengar, J. Tomasi, V. Barone, B. Mennucci, M. Cossi, G. Scalmani, N. Rega, G. A. Petersson, H. Nakatsuji, M. Hada, M. Ehara, K. Toyota, R. Fukuda, J. Hasegawa, M. Ishida, T. Nakajima, Y. Honda, O. Kitao, H. Nakai, M. Klene, X. Li, J. E. Knox, H. P. Hratchian, J. B. Cross, C. Adamo, J. Jaramillo, R. Gomperts, R. E. Stratmann, O. Yazyev, A. J. Austin, R. Cammi, C. Pomelli, J. W. Ochterski, P. Y. Ayala, K. Morokuma, G. A. Voth, P. Salvador, J. J. Dannenberg, V. G. Zakrzewski, S. Dapprich, A. D. Daniels, M. C. Strain, O. Farkas, D. K. Malick, A. D. Rabuck, K. Raghavachari, J. B. Foresman, J. V. Ortiz, Q. Cui, A. G. Baboul, S. Clifford, J. Cioslowski, B. B. Stefanov, G. Liu, A. Liashenko, P. Piskorz, I. Komaromi, R. L. Martin, D. J. Fox, T. Keith, M. A. Al-Laham, C. Y. Peng, A. Nanayakkara, M. Challacombe, P. M. W. Gill, B. Johnson, W. Chen, M. W. Wong, C. Gonzalez, J. A. Pople, *Gaussian 03*, Revision C.02, Gaussian, Inc., Wallingford CT, **2004**.
- [22] a) A. D. Becke, *J. Chem. Phys.* **1993**, 98, 5648–5652; b) C. Lee, W. Yang, R. G. Parr, *Phys. Rev. B* **1988**, 37, 785–789.
- [23] M. Dolg, U. Wedig, H. Stoll, H. Preuss, *J. Chem. Phys.* **1987**, 86, 866–872.
- [24] W. J. Hehre, L. Radom, P. v R. Schleyer, J. A. Pople, *Ab Initio Molecular Orbital Theory*; John Wiley & Sons, Inc., New York, **1986**, and references cited therein.
- [25] M. Yamana, A. Inagaki, E. Nakamura, *J. Comput. Chem.* **2003**, 24, 1401–1409.
- [26] a) K. Fukui, *Acc. Chem. Res.* **1981**, 14, 363–368; b) C. Gonzalez, H. B. Schlegel, *J. Chem. Phys.* **1989**, 90, 2154–2161; c) C. Gonzalez, H. B. Schlegel, *J. Phys. Chem.* **1990**, 94, 5523–5527.
- [27] a) J. Bigeleisen, M. G. Mayer, *J. Chem. Phys.* **1947**, 15, 261–267; b) J. Bigeleisen, M. Wolfsberg, *Adv. Chem. Phys.* **1958**, 1, 15–76.
- [28] A. P. Scott, L. Radom, *J. Phys. Chem.* **1996**, 100, 16502–16513.
- [29] a) A. E. Reed, R. B. Weinstock, F. Weinhold, *J. Chem. Phys.* **1985**, 83, 735–746; b) A. E. Reed, L. A. Curtiss, F. Weinhold, *Chem. Rev.* **1988**, 88, 899–926; c) NBO Version 3.1 in the Gaussian 03 package implemented by E. D. Glendening, A. E. Reed, J. E. Carpenter, F. Weinhold, University of Wisconsin: Madison, WI, **1990**.